

Supramolecular Synthesis of Organic Laminates with Affinity for Aromatic Guests: A New Class of Clay Mimics

Kumar Biradha, Dorothy Dennis, Verna A. MacKinnon, C. V. Krishnamohan Sharma, and Michael J. Zaworotko*

Contribution from the Department of Chemistry, The University of Winnipeg, 515 Portage Avenue, Winnipeg, Manitoba, Canada, R3B 2E9

Received October 29, 1997. Revised Manuscript Received August 17, 1998

Abstract: Single-crystal X-ray diffraction analysis of 25 supramolecular laminate structures formed from reaction of trimesic acid or trimellitic acid with 2 equiv of *N,N*-dibenzylamine reveals an ability to incorporate aromatic guest molecules irrespective of their size and electronic nature. The guest molecules included are nitrobenzene, anisole, veratrole, 1,4-dimethoxybenzene, 1,3,5-trimethoxybenzene, *m*-xylene, mesitylene, tetramethylbenzene, pentamethylbenzene, hexamethylbenzene, *N,N*-dibenzylamine, naphthalene, 1-methylnaphthalene, pyrene, and ferrocene. The acid moieties and ammonium cations reproducibly form charge-assisted 2D hydrogen-bonded layers with pendant benzyl groups above and below the layers. In the absence of guest molecules, interdigitation of benzyl groups is observed. Guest molecules interact with the laminates via a plethora of aromatic edge-to-face and face-to-face interactions. The unit cell lengths are based upon multiples of $\sim 12 \times 17 \times 21$ Å. The 12-Å dimension represents the approximate interlayer separation whereas the 17×21 Å dimensions represent the hydrogen-bonded layer.

Introduction

Crystal engineering continues to offer the intriguing promise of rational development of a new generation of functional solids that have been designed from first principles. The relatively recent rise in interest in this concept¹ owes much to advancements in supramolecular chemistry, recognition, understanding, and exploitation of *supramolecular synthons*² and, implicitly, the concept of supramolecular synthesis of solids. A property of solids that has attracted considerable attention from materials chemists and crystal engineers is the ability of a solid to adsorb and/or desorb guest molecules. Clays, via intercalation between 2D layers, and zeolites, which contain channels and cavities because of rigid 3D frameworks, are natural prototypes that are of considerable commercial interest because of their widespread applications in separations and catalysis.³ There already exist several examples of metal–organic^{4,5} and organic^{6–8} zeolite mimics which reversibly incorporate small-molecule or organic guests and there are also metal–organic^{9,10} and organic¹¹ clay mimics. 2D frameworks (clay mimics) complement their rigid

3D counterparts (zeolite mimics) as they are often capable of varying their interlayer separation in order to accommodate guest molecules according to the structural and steric requirements of the guest.¹² Furthermore, the presence of the cavities or channels in the apohost is not a prerequisite for these materials to incorporate guest molecules and, depending upon chemical structure, they are capable of incorporating either hydrophilic or hydrophobic guests.

Recently, organic salts have also been employed in the design of layered and/or porous solids.¹³ Interestingly, the analogy with clays extends to the concept of pillaring the layered networks.^{13e} Organic salts are likely to be more useful than molecular analogues for several reasons: they promise predictability because of their tendency to form robust charge-assisted H-bonded supramolecular synthons; these synthons tend to afford greater thermal stability than their neutral analogues;¹⁴ they are inherently modular in nature; i.e., a simple change of

(1) (a) Desiraju, G. R. *Crystal Engineering: The Design of Organic Solids*; Elsevier: Amsterdam, 1989. (b) Etter, M. C. *Acc. Chem. Res.* **1990**, *23*, 120–126. (c) Maddox, J. *Nature* **1988**, *335*, 201. (d) Ball, P. *Nature* **1996**, *381*, 648.

(2) (a) Desiraju, G. R. *Angew. Chem., Int. Ed. Engl.* **1995**, *34*, 2311–2327. (b) Lehn, J.-M. *Supramolecular Chemistry*; VCH: Weinheim, 1995. (c) Bernstein, J.; Davis, R. E.; Shimon, L.; Chang, N.-L. *Angew. Chem., Int. Ed. Engl.* **1995**, *34*, 1555. (d) Hosseini, M. W.; DeCian, A. *Chem. Commun.* **1998**, 727–734.

(3) Liebau, F. *Structural Chemistry of Silicates*; Springer-Verlag: Berlin, 1985.

(4) (a) Li, H.; Davis, C. E.; Groy, T. L.; Kelley, D. G.; Yaghi, O. M. *J. Am. Chem. Soc.* **1998**, *120*, 0, 2186–2187. (b) Yaghi, O. M.; Li, G.; Li, H. *Nature* **1995**, *378*, 703–705.

(5) Venkataraman, D.; Gardner, G. B.; Lee, S.; Moore, J. S. *J. Am. Chem. Soc.* **1995**, *117*, 11600–11601.

(6) Kondo, M.; Yoshitomi, T.; Seki, K.; Matsuzaka, H.; Kitagawa S. *Angew. Chem., Int. Ed. Engl.* **1997**, *36*, 1725–1727.

(7) Brunet, P.; Simard, M.; Wuest, J. D. *J. Am. Chem. Soc.* **1997**, *119*, 2737.

(8) (a) Endo, K.; Sawaki, T.; Koyanagi, M.; Kobayashi, K.; Masuda, H.; Aoyama, Y. *J. Am. Chem. Soc.* **1995**, *117*, 8341–8352. (b) Endo, K.; Ezuhara, T.; Koyanagi, M.; Masuda, H.; Aoyama, Y. *J. Am. Chem. Soc.* **1997**, *119*, 499–505.

(9) Shimizu, G. K. H.; Enright, G. D.; Ratcliffe, C. I.; Ripmeester, J. A.; Wayner, D. D. M. *Angew. Chem., Int. Ed. Engl.* **1998**, *37*, 1407–1409.

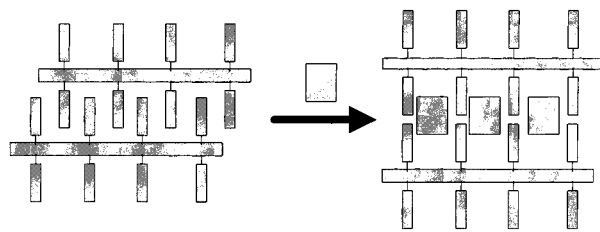
(10) (a) Fujita, M.; Kwon, Y. J.; Washijiu, S.; Ogura, K. *J. Am. Chem. Soc.* **1994**, *116*, 1151–1152. (b) Biradha, K.; Dennis, D.; MacKinnon, V. A.; Seward, C.; Zaworotko, M. J. In *Current Challenges on Large Scale Supramolecular Assemblies*; Tsoucaris, G., Ed.; NATO ARW; Kluwer Academic Publishers: Dordrecht, The Netherlands, 1998.

(11) Coleman, A. W.; Bott, S. G.; Morley, S. D.; Means, C. M.; Robinson, K. D.; Zhang, H.; Atwood, J. L. *Angew. Chem., Int. Ed. Engl.* **1988**, *27*, 1361.

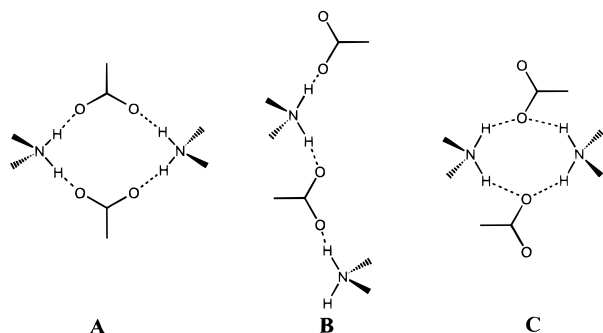
(12) (a) Müller, A.; Reuter, H.; Dillinger, S. *Angew. Chem., Int. Ed. Engl.* **1995**, *34*, 2328–2361. (b) Losier, P.; Zaworotko, M. J. *Angew. Chem., Int. Ed. Engl.* **1996**, *35*, 2779–2782.

(13) (a) Russell, V. A.; Etter, M. C.; Ward, M. D. *J. Am. Chem. Soc.* **1994**, *116*, 1941–1952. (b) Russell, V. A.; Etter, M. C.; Ward, M. D. *Chem. Mater.* **1994**, *6*, 1206–1217. (c) Russell, V. A.; Ward, M. D. *J. Mater. Chem.* **1997**, *7*, 1123–1133. (d) Russell, V. A.; Evans, C. C.; Li W.; Ward, M. D. *Science* **1997**, *276*, 575. (e) Swift, J. A.; Pivovar, A. M.; Reynolds, A. M.; Ward, M. D. *J. Am. Chem. Soc.* **1998**, *120*, 5887–5894.

Scheme 1



the ancillary functional groups of either the cation or the anion will generate new materials without altering the basic supramolecular synthons. The supramolecular synthons (A–C) that



form between carboxylate anions and ammonium cations are potentially important tools for the design of ionic organic materials because of their ubiquity and the complementary nature of the strong hydrogen bond donors of the cations and the strong hydrogen bond acceptors of the anions.¹⁵ Supramolecular synthons **A** and **B** are similar to those of the carboxylic acid dimer and catamer, respectively, while synthon **C** contains bifurcated interactions.

Trimesic acid (H_3TMA) and trimellitic acid (H_3TML) are two inexpensive and thermally and chemically robust carboxylic acids with exodentate functionality in two dimensions. Therefore, they represent ideal templates for generation of 2D hydrogen-bonded arrays.^{15–20} We have demonstrated that the salt $[NR_2H]_3[TMA]$ ($R = \text{cyclohexyl}$) is capable of forming a honeycomb network with large cavities that are encapsulated by the R groups of cations, thereby avoiding interpenetration of the honeycomb networks.¹⁵ We also reported that similar salts but of different stoichiometry, $[R_2NH_2]_2[HTMA]$ and $[R_2NH_2]_2[HTML]$ ($R = \text{propyl, hexyl, octyl, decyl}$), generate interdigitated supramolecular laminates which have poor ability to incorporate guest molecules.¹⁷ It occurred to us that for $R = \text{benzyl}$ interdigitation would be less favored from a steric perspective and would therefore facilitate incorporation of solvent or aromatic guest molecules (Scheme 1).

In this contribution, we describe the ability of the compounds $[(PhCH_2)_2NH_2]_2[HTMA]$ (**I**) and $[(PhCH_2)_2NH_2]_2[HTML]$ (**II**) to enclathrate aromatic guest molecules irrespective of their size, shape, and functionality. These compounds can be regarded

(14) (a) Aakeröy, C. B.; Nieuwenhuysen, M. J. *Am. Chem. Soc.* **1994**, *116*, 10983. (b) Aakeröy, C. B. *Acta Crystallogr.* **1997**, *B53*, 569.

(15) Melendez, R. E.; Sharma, C. V. K.; Zaworotko, M. J.; Bauer, C.; Rogers, R. D. *Angew. Chem., Int. Ed. Engl.* **1996**, *35*, 2213.

(16) Herbstein, F. H. *Top. Curr. Chem.* **1987**, *140*, 107–139.

(17) Sharma, C. V. K.; Bauer, C. B.; Rogers, R. D.; Zaworotko, M. J. *Chem. Commun.* **1997**, 1559.

(18) Coe, S.; Kane, J. J.; Nguyen, T. L.; Toledo, L. M.; Winger, E.; Fowler, F. W.; Lauher, J. W. *J. Am. Chem. Soc.* **1997**, *119*, 86–93.

(19) Pedireddi, V. R.; Jones, W.; Chorlton, A. P.; Docherty, R. *Chem. Commun.* **1996**, 997.

(20) Hamuro, Y.; Geib, S. J.; Hamilton, A. D. *J. Am. Chem. Soc.* **1996**, *118*, 7529.

as examples of organic supramolecular laminates that, although they are structurally related to clays, are inherently hydrophobic and have a strong affinity toward aromatic guests.

Results and Discussion

If **I** or **II** is crystallized in the absence of aromatic molecules it forms interdigitated supramolecular laminates with relatively short interlayer separations. Solvent molecules can be incorporated by H-bonding interactions. However, if **I** or **II** is crystallized in the presence of any of a range of aromatic guest molecules, then the aromatic molecules intercalate and larger interlayer separations are observed.²¹ Salient crystallographic details for the 25 complexes reported herein are presented in Table 1.

Solvated Hosts. **I** and **II** each form two complexes with solvent molecules. **I** forms solvates with H_2O (**1a**) and MeOH (**1b**), whereas **II** forms solvates with EtOH (**2a**) and MeCN (**2b**). All four compounds exhibit 2D H-bonded layers in which the benzyl groups orient above and below the layers. The packing of these layers affords a supramolecular laminate structure in which the benzyl groups are interdigitated (Figure 1). Although these four complexes exhibit similar supramolecular laminate structures, they are not identical. Specifically, there is variation in the connectivity within the H-bonded layers (Figure 2) and in the manner in which solvent molecules are incorporated.

1a and **1b** form flat H-bonded layers in which the solvent molecules directly participate in the H-bonded network (Figure 2a and b). In **1a**, the layer is constituted by three H-bonded rings formed by 14 (3 H-bonds), 18 (5 H-bonds), and 20 atoms (6 H-bonds). In **1b**, it is composed of two types of H-bonded rings, a 22-membered (6 H-bonds) and a 24-membered (6 H-bonds) ring. The methyl groups of the MeOH molecules point to only one side of the layer, thereby precluding the presence of an inversion center within the layer. However, the layers pack in a centrosymmetric fashion. Alternate layers contain either solvent or benzyl groups (Figure 1b). As would be expected, the interlayer separation of the interdigitated layers is less than that of the layers that contain solvent (7.6 vs 9.4 Å).

2a and **2b** each contain two crystallographically independent sets of cations and anions. **2a** contains two types of H-bonded layer (Figure 2c). The first is flat and constituted of an array of cyclic H-bonded rings formed by 36 atoms (8 H-bonds) whereas the other is corrugated and consists of a series of 38-membered cyclic H-bonded rings (10 H-bonds). In the latter, OH groups of EtOH molecules are involved in H-bond formation and the ethyl groups point to only one side of the layer. The layers pack so that alternate layers either interdigitate or contain EtOH molecules (Figure 1c).

2b generates only one type of H-bonded layer (Figure 2d). It is composed of two types of H-bonded rings formed by 42 (8 H-bonds) and 30 atoms (8 H-bonds), respectively. Hexameric aggregates of HTMA moieties propagate throughout the layer. The H-bonded sheets are corrugated and pack (Figure 1d) so that crests and troughs point toward each other. This type of packing generates alternately large and small cavities. The large cavities are occupied by interdigitated benzyl groups, whereas the small cavities are occupied by MeCN molecules which do not participate in the H-bonded network.

(21) Interestingly, the doubly deprotonated salt of 1,2,4,5-benzenetetracarboxylic acid (pyromellitic acid) with N,N -dibenzylamine also resulted in an interdigitated lamellar architecture with an interlayer separation of 8.4 Å. However, our attempts to prepare host–guest complexes of this system have not yet been successful.

Table 1. Crystallographic Parameters (a) Solvated Host Complexes of **I** and **II**

(a) Solvated Host Complexes of I and II									
	1a	1b	2a	2b		1a	1b	2a	2b
formula	C ₃₇ H ₃₈ N ₂ O ₇	C ₃₈ H ₄₀ N ₂ O ₇	C ₃₈ H ₃₉ N ₂ O _{6.5}	C ₃₈ H _{37.5} N _{2.5} O ₆	<i>F</i> (000)	1320	676	2661.09	2648
mol wt	622.69	636.74	627.22	625.22	λ (Mo K α)	0.710 73	0.710 73	0.710 73	0.710 73
temp (K)	193	293	293	193	2θ range (deg)	1.68–27.98	0–24.95	0–22.50	1.31–25
system	monoclinic	triclinic	monoclinic	monoclinic	h_{\min}/h_{\max}	$-14 \leq h \leq 14$	$-9 \leq h \leq 10$	$-20 \leq h \leq 20$	$-22 \leq h \leq 17$
space group	<i>P</i> ₂ ₁ / <i>n</i>	<i>P</i> -1	<i>P</i> ₂ ₁ / <i>a</i>	<i>P</i> ₂ ₁ / <i>n</i>	k_{\min}/k_{\max}	$-21 \leq k \leq 24$	$0 \leq k \leq 14$	$0 \leq k \leq 11$	$-25 \leq k \leq 26$
<i>a</i> (Å)	11.0380(5)	8.804(2)	19.0094(21)	17.1045(8)	l_{\min}/l_{\max}	$19 \leq l \leq 20$	$-19 \leq l \leq 19$	$0 \leq l \leq 35$	$-26 \leq l \leq 27$
<i>b</i> (Å)	18.3003(9)	11.803(3)	10.9107(11)	20.5394(10)	no. of measd rflns	7609	5816	9070	11771
<i>c</i> (Å)	16.2330(8)	16.748(4)	33.232(7)	20.8923(10)	no. of unique rflns	5545	4141	4204	5184
α (deg)	90	83.76(6)	90	90	no. of refined params	427	424	170	831
β (deg)	95.6330(10)	81.61(4)	91.300(13)	113.4180(10)	GOF on <i>F</i> ²	0.885	7.43	0.82	0.732
γ (deg)	90	74.48(4)	90	90	<i>R</i> ₁ (on <i>F</i> , <i>I</i> > 2 σ (<i>I</i>))	0.0403	0.076	0.059	0.0528
<i>V</i> (Å ³)	3263.2(3)	4312.9(6)	6890.8(17)	6735.2(6)	w <i>R</i> ₂ (on <i>F</i> ² , all data)	0.1303	0.081	0.058	0.1644
<i>Z</i>	4	2	8	8					
(b) Host–Guest Complexes of I									
	1c	1d	1e	1f	1g	1h	1i	1j	
formula	C ₄₇ H ₅₀ N ₂ O ₆	C ₄₈ H ₅₂ N ₂ O ₆	C ₄₆ H ₄₈ N ₂ O ₆	C ₄₆ H ₄₈ N ₂ O ₉	C _{49.50} H ₄₆ N ₂ O ₆	C _{50.75} H _{48.5} N ₂ O ₆	C _{45.67} H ₄₈ N ₂ O _{8.33}	C _{40.50} H ₄₁ N ₂ O ₇	
mol wt	847.87	752.94	724.86	771.86	763.88	777.86	758.20	667.76	
temp (K)	293	293	293	193	193	193	193	193	
system	monoclinic	monoclinic	monoclinic	triclinic	triclinic	monoclinic	monoclinic	monoclinic	
space group	<i>P</i> ₂ ₁ / <i>c</i>	<i>P</i> ₂ ₁ / <i>c</i>	<i>P</i> ₂ ₁ / <i>c</i>	<i>P</i> -1	<i>P</i> -1	<i>P</i> ₂ ₁ / <i>n</i>	<i>P</i> ₂ ₁ / <i>c</i>	<i>P</i> ₂ ₁ / <i>c</i>	
<i>a</i> (Å)	12.1443(10)	12.0255(17)	21.806(2)	11.8148(6)	16.9682(8)	16.9394(4)	11.5765(6)	16.8747(8)	
<i>b</i> (Å)	21.9150(12)	16.8955(14)	11.7442(10)	21.7742(11)	21.6307(11)	21.839(2)	49.905(3)	22.4446(10)	
<i>c</i> (Å)	16.9258(19)	21.714(4)	33.299(3)	33.100(2)	23.7573(12)	23.775(2)	21.5054(13)	38.311(2)	
α (deg)	90	90	90	89.975(1)	93.9670(10)	90	90	90	
β (deg)	97.105(21)	93.88(4)	90.730(2)	87.332(1)	99.1010(10)	98.040(2)	90.929(1)	91.538(1)	
γ (deg)	90	90	90	85.118(1)	90.0400(10)	90	90	90	
<i>V</i> (Å ³)	4470.1(7)	4401.7(10)	8526.9(12)	8475.1(8)	8588.7(7)	8708.8(11)	12422.6(12)	14504.9(12)	
<i>Z</i>	4	4	8	8	8	8	12	16	
<i>F</i> (000)	847.87	1608.61	3080	3272	3232	3272	4820	5612	
λ (Mo K α)	0.710 73	0.710 73	0.710 73	0.710 73	0.710 73	0.710 73	0.710 73	0.710 73	
2θ range (deg)	0.99–23.54	0.99–25.00	0.93–27.88	0.94–25.00	0.87–28.79	1.27–25.00	0.82–25.00	1.05–25.00	
h_{\min}/h_{\max}	$-13 \leq h \leq 13$	$-14 \leq h \leq 14$	$-16 \leq h \leq 28$	$-15 \leq h \leq 7$	$-22 \leq h \leq 22$	$-22 \leq h \leq 19$	$-15 \leq h \leq 9$	$-20 \leq h \leq 22$	
k_{\min}/k_{\max}	$0 \leq k \leq 25$	$0 \leq k \leq 20$	$-15 \leq k \leq 15$	$-28 \leq k \leq 28$	$-28 \leq k \leq 17$	$-28 \leq k \leq 26$	$-65 \leq k \leq 57$	$-24 \leq k \leq 29$	
l_{\min}/l_{\max}	$0 \leq l \leq 19$	$0 \leq l \leq 25$	$-43 \leq l \leq 37$	$-43 \leq l \leq 40$	$-30 \leq l \leq 31$	$-19 \leq l \leq 31$	$-20 \leq l \leq 28$	$-50 \leq l \leq 49$	
no. of measd rflns	7249	7934	19448	27420	35294	15091	21508	25316	
no. of unique rflns	6999	7726	4633	16971	21671	5318	11030	10906	
no. of refined params	547	507	979	2041	2047	1023	1568	1821	
GOF on <i>F</i> ²	2.33	4.34	0.938	0.997	1.013	1.009	1.000	1.010	
<i>R</i> ₁ (on <i>F</i> , <i>I</i> > 2 σ (<i>I</i>))	0.135 Rf	0.061 Rf	0.1264	0.1001	0.1065	0.1434	0.0761	0.0954	
w <i>R</i> ₂ (on <i>F</i> ² , all data)	0.140Rw	0.054 Rw	0.3109	0.2651	0.3245	0.3849	0.1715	0.2845	
(c) Host–Guest Complexes of II									
	2c	2d	2e	2f	2g	2h	2i		
formula	C ₅₁ H ₅₁ N ₃ O ₆	C ₄₈ H ₄₈ N ₂ O ₆	C ₄₇ H ₅₀ N ₂ O ₆	C ₄₈ H ₅₂ N ₂ O ₆	C _{24.5} H ₂₇ N ₁ O ₃	C _{22.5} H ₂₃ N ₁ O ₄	C _{26.5} H ₂₃ N ₁ O ₃		
mol wt	801.97	746.87	737.88	1505.90	766.94	742.87	806.94		
temp (K)	293	293	193	193	293	293	293		
system	monoclinic	monoclinic	triclinic	orthorhombic	orthorhombic	orthorhombic	orthorhombic		
space group	<i>P</i> ₂ ₁ / <i>c</i>	<i>P</i> ₂ ₁ / <i>c</i>	<i>P</i> -1	<i>Ab</i> a2	<i>Cm</i> ca	<i>Cc</i> mb	<i>Cc</i> mb		
<i>a</i> (Å)	12.788(3)	12.1096(9)	18.6410(9)	21.3680(10)	24.699(2)	17.0677(10)	17.0774(14)		
<i>b</i> (Å)	21.346(4)	21.079(2)	22.6285(12)	17.0003(8)	17.0919(14)	24.167(2)	24.5676(21)		
<i>c</i> (Å)	17.013(10)	17.1650(13)	23.9918(12)	24.1545(12)	21.437(2)	21.4778(13)	21.3503(19)		
α (deg)	90	90	107.6380(10)	90	90	90	90		
β (deg)	99.78(3)	100.159(2)	102.7690(10)	90	90	90	90		
γ (deg)	90	90	110.3430(10)	90	90	90	90		
<i>V</i> (Å ³)	4577(3)	4312.9(6)	8418.1(7)	8774.4(7)	9049.8(13)	8859.1(9)	8957.5(13)		
<i>Z</i>	4	4	8	8	8	8	8		
<i>F</i> (000)	1704	1584	3144	3016	3280	3160	3409.30		
λ (Mo K α)	0.710 73	0.710 73	0.710 73	0.710 73	0.710 73	0.710 73	0.710 73		
2θ range (deg)	0–22.45	1.54–25.00	0.96–25.00	1.69–25.00	1.65–25.00	1.68–25.00	0–22.9		
h_{\min}/h_{\max}	$-13 \leq h \leq 13$	$-14 \leq h \leq 15$	$-12 \leq h \leq 24$	$-26 \leq h \leq 28$	$-28 \leq h \leq 31$	$-22 \leq h \leq 21$	$0 \leq h \leq 18$		
k_{\min}/k_{\max}	$0 \leq k \leq 22$	$-27 \leq k \leq 15$	$-29 \leq k \leq 27$	$-22 \leq k \leq 16$	$-22 \leq k \leq 21$	$-31 \leq k \leq 31$	$0 \leq k \leq 26$		
l_{\min}/l_{\max}	$0 \leq l \leq 18$	$-22 \leq l \leq 22$	$-31 \leq l \leq 29$	$-31 \leq l \leq 31$	$-27 \leq l \leq 26$	$-22 \leq l \leq 28$	$0 \leq l \leq 23$		
no. of measd rflns	6184	7478	26314	7590	4079	4026	4359		
no. of unique rflns	5951	2691	8743	5311	1876	2280	3195		
no. of refined params	541	474	1973	469	290	293	304		
GOF on <i>F</i> ²	3.77	0.917	0.947	0.978	1.036	1.043	2.90		
<i>R</i> ₁ (on <i>F</i> , <i>I</i> > 2 σ (<i>I</i>))	0.093	0.0936	0.1083	0.1178	0.0804	0.1075	0.056		
w <i>R</i> ₂ (on <i>F</i> ² , all data)	0.077	0.3284	0.3282	0.3803	0.1948	0.3657	0.051		

Table 1 (Continued)

	2j	2k	2l	2m	2n	2o
formula	C ₄₇ H ₄₆ N ₂ O ₆ Fe ₁	C ₄₉ H ₅₁ N ₂ O ₉	C ₄₉ H ₅₁ N ₂ O ₆	C ₄₉ H ₅₂ N ₂ O ₆	C _{38.75} H ₃₈ N ₂ O _{6.25}	C _{47.5} H _{44.75} N _{3.75} O _{9.5}
mol wt	791.72	811.92	763.92	764.39	631.71	820.15
temp (K)	193	193	210	193	193	198
system	monoclinic	orthorhombic	orthorhombic	monoclinic	triclinic	triclinic
space group	<i>P2₁/n</i>	<i>Aba2</i>	<i>Aba2</i>	<i>P2₁/c</i>	<i>P1</i>	<i>P-1</i>
<i>a</i> (Å)	14.0860(8)	21.4194(13)	21.176(2)	12.1455(17)	12.0485(7)	17.0889(10)
<i>b</i> (Å)	20.9125(12)	17.1608(10)	17.0701(11)	63.295(3)	16.6565(10)	21.4172(12)
<i>c</i> (Å)	15.1690(2)	24.0506(14)	23.848(2)	17.1164(9)	18.2126(11)	24.602(2)
α (deg)	90	90	90	90	99.7150(10)	106.5680(10)
β (deg)	108.7710(10)	90	90	99.1460(10)	94.9320(10)	95.6640(10)
γ (deg)	90	90	90	90	107.2890(10)	90.4050(10)
<i>V</i> (Å ³)	4230.7(4)	8840.4(9)	8620.3(10)	12990.9(12)	3403.6(4)	8582.4(9)
<i>Z</i>	4	8	8	12	4	8
<i>F</i> (000)	1668	3448	3256	4890	1338	3456
λ (Mo Kα)	0.710 73	0.710 73	0.710 73	0.710 73	0.710 73	0.710 73
2(range) (deg)	1.72–22.50	1.69–28.18	1.71–28.62	0.64–25.00	1.15–27.90	0.87–27.97
<i>h</i> _{min} / <i>h</i> _{max}	−18 ≤ <i>h</i> ≤ 18	−25 ≤ <i>h</i> ≤ 27	−27 ≤ <i>h</i> ≤ 26	−15 ≤ <i>h</i> ≤ 15	−15 ≤ <i>h</i> ≤ 11	−15 ≤ <i>h</i> ≤ 22
<i>k</i> _{min} / <i>k</i> _{max}	−19 ≤ <i>k</i> ≤ 26	−22 ≤ <i>k</i> ≤ 14	−20 ≤ <i>k</i> ≤ 19	−83 ≤ <i>k</i> ≤ 79	−19 ≤ <i>k</i> ≤ 21	−24 ≤ <i>k</i> ≤ 27
<i>l</i> _{min} / <i>l</i> _{max}	−19 ≤ <i>l</i> ≤ 16	−31 ≤ <i>l</i> ≤ 30	−21 ≤ <i>l</i> ≤ 32	−10 ≤ <i>l</i> ≤ 22	−22 ≤ <i>l</i> ≤ 23	−31 ≤ <i>l</i> ≤ 32
no. of measd reflns	5494	9675	7807	22294	17287	36581
no. of unique reflns	3823	4670	3866	8859	13395	15223
no. of refined params	480	548	522	1520	1710	2255
GOF on <i>F</i> ²	1.110	1.033	0.947	0.959	1.039	0.993
<i>R</i> ₁ (on <i>F</i> , <i>I</i> > 2σ(<i>I</i>))	0.1325	0.08594	0.0644	0.1099	0.0487	0.0839
w <i>R</i> ₂ (on <i>F</i> ² , all data)	0.3525	0.1478	0.1623	0.3487	0.1476	0.2507

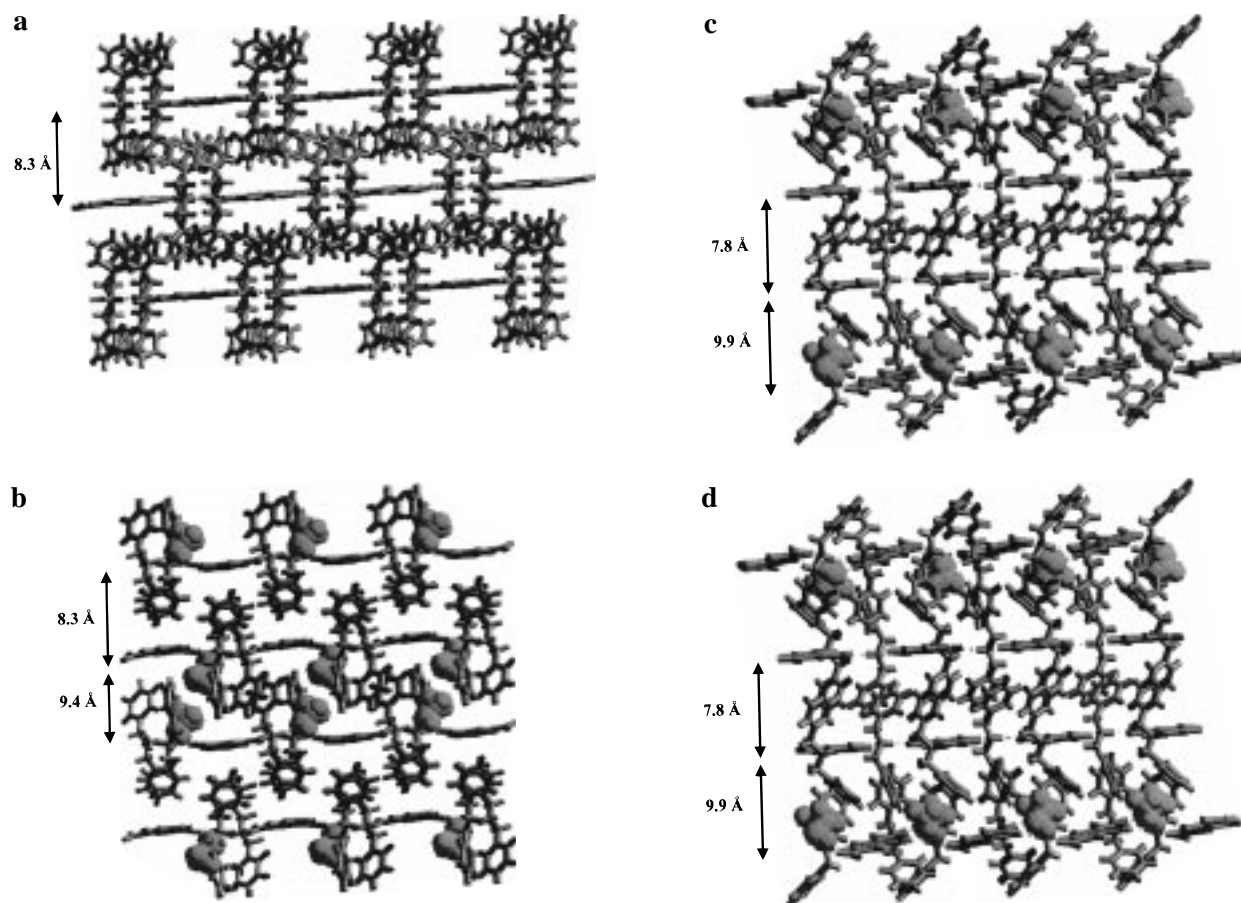


Figure 1. Supramolecular laminates (a) 1a, (b) 1b, (c) 1c, and (d) 1d. Solvent molecules are presented in space-filling mode.

Host–Guest Complexes. We have structurally characterized 8 and 13 host–guest complexes of **I** and **II**, respectively. The guest molecules included by **I** are tetramethylbenzene (**1c**), pentamethylbenzene (**1d**), 1,3,5-trimethylbenzene (**1e**), 1,3,5-trimethoxybenzene (**1f**), naphthalene (**1g**) 1-methylnaphthalene (**1h**), veratrole (**1i**), and anisole (**1j**). The guest molecules included by **II** are *N,N*-dibenzylamine (**2c**), 1-methylnaphthalene

(**2d**), tetramethylbenzene (**2e**), pentamethylbenzene (**2f**), hexamethylbenzene (**2g**), veratrole (**2h**), pyrene (**2i**), ferrocene (**2j**), 1,4-dimethoxybenzene (**2k**), *m*-xylene (**2l**), mesitylene (**2m**), anisole (**2n**), and nitrobenzene (**2o**). The host–guest ratios, interlayer separations, and percent of guest with respect to host by mass are compared for these compounds in Table 2. Although all 21 of the complexes form supramolecular lami-

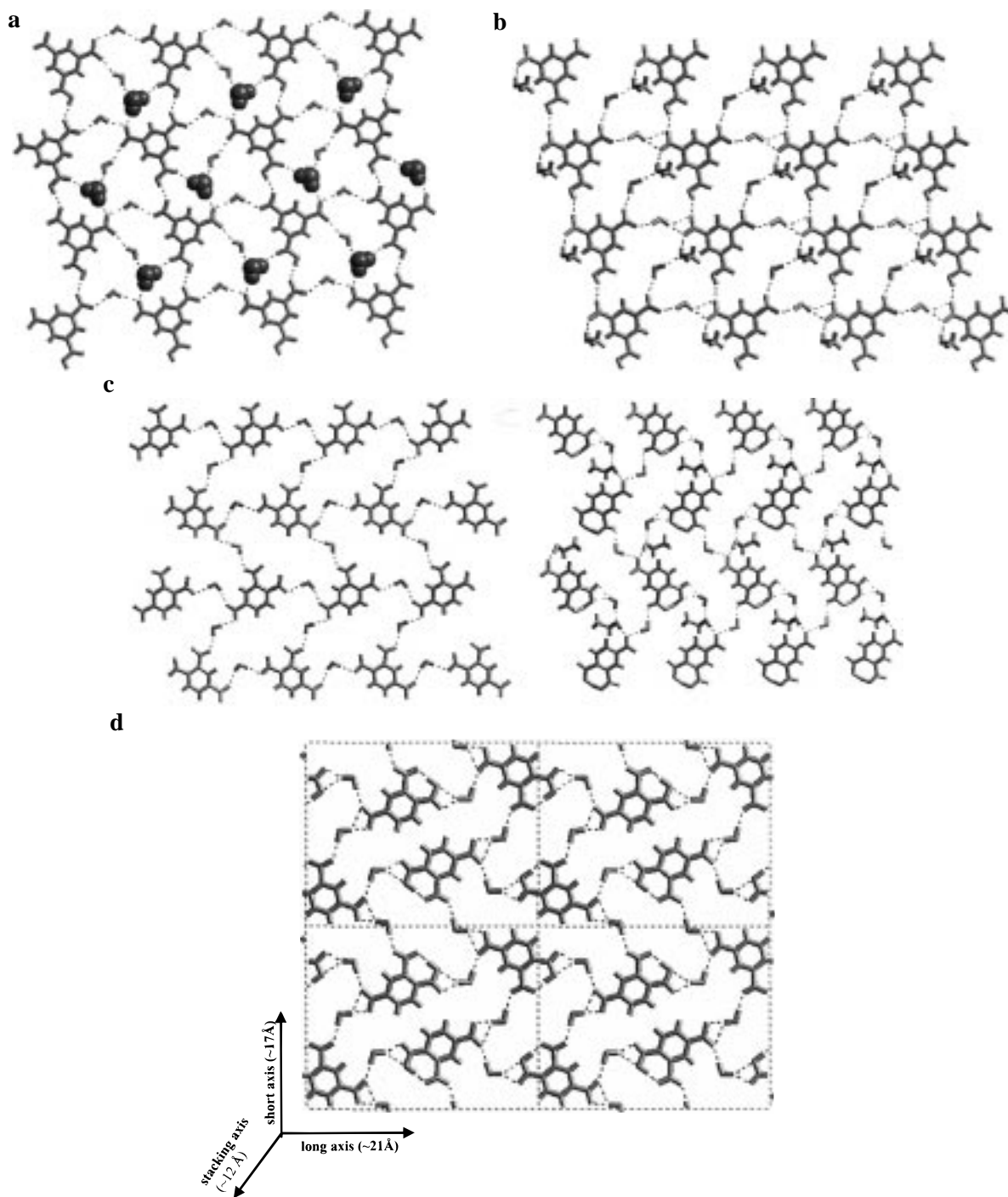


Figure 2. H-bonded networks in (a) **1a**, (b) **1b**, (c) **1c**, and (d) **1d**. Benzyl groups are omitted for the sake of clarity. Note the direct participation of solvent molecules in the H-bonded networks in **1a**, **1b**, and **1c**.

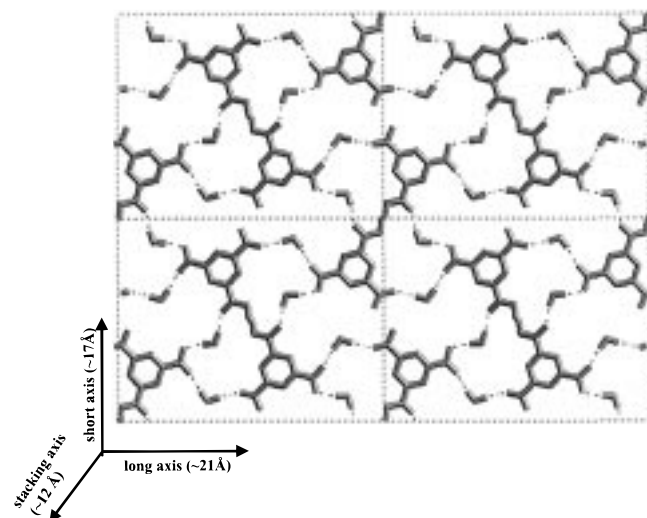
nated architectures, there is some variation in the geometry of the hydrogen-bonded layer and in the manner in which guest molecules are incorporated. In general, guest molecules are surrounded by benzyl groups which form a plethora of aromatic C–H $\cdots\pi$ interactions.²² The unit cell lengths of 17 of the complexes are multiples of $\sim 12 \times 17 \times 21$ Å (stacking axis, short axis, and long axis, respectively). The length of the stacking axis represents the approximate interlayer separation. A doubling of the length of the stacking axis occurs when adjacent layers are not related by translation. Multiples of short

and long axes occur because of differences in the arrangement of guest molecules between benzyl groups. In effect, guest molecules and/or benzyl groups do not necessarily repeat with the asymmetric unit of the H-bonded layer. The crystal structures might be classified on the basis of the stacking axis as being of one of two types: (1) identical packing of adjacent layers (i.e., related by translation); (2) adjacent layers which are different from each other (cf. the solvated compounds **1a**, **1b**, **2a**, **2b**, **1j**, and **2o**). The H-bonded sheets can be either flat or corrugated. A detailed analysis of the interactions between benzyl groups of the host and the guest molecules revealed that the packing of the structures are essentially identical if the host–

(22) (a) Jorgensen, W. L.; Severance, D. L. *J. Am. Chem. Soc.* **1990**, *112*, 4768. (b) Shetty, A. S.; Zhang J.; Moore, J. S. *J. Am. Chem. Soc.* **1996**, *118*, 1019. (c) Hunter, C. A. *Chem. Soc. Rev.* **1994**, *23*, 101.

Table 2. Some Important Details of Host–Guest Complexes

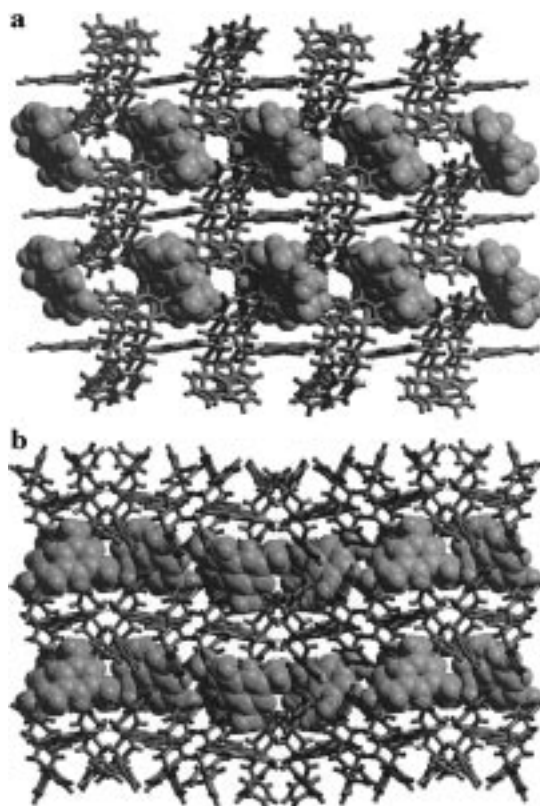
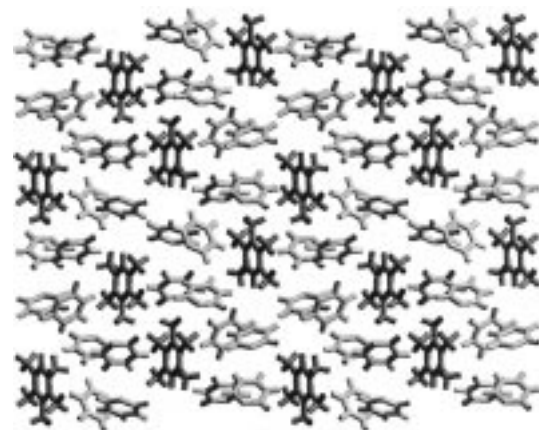
compound	host:guest	separation (Å)	%guest by mass	sheet
(a) Host–Guest Complexes of I				
1c	1:1	12.1	18.2	corrugated
1d	1:1	12.2	19.7	corrugated
1e	1:1	11.7	16.6	corrugated
1f	1:1	11.8	21.8	corrugated
1g	4:5	11.8	21.0	corrugated
1h	4:5	11.9	22.7	corrugated
1i	3:3:1EtOH	11.6	20.2	corrugated
1j	2:1:1H ₂ O	9.3, 9.8	9.4	corrugated
(b) Host–Guest Complexes of II				
2c	1:1	12.9	24.6	flat
2d	1:1	12.1	19.0	corrugated
2e	1:1	12.1	18.2	corrugated
2f	1:1	12.1	19.7	flat
2g	1:1	12.3	21.2	flat
2h	1:1	12.1	20.2	flat
2i	1:1	12.3	25.1	flat
2j	1:1	12.2	16.0	corrugated
2k	1:1.5	12.0	25.5	corrugated
2l	1:1.5	11.9	20.8	flat
2m	3:4	12.1	20.9	corrugated
2n	4:1	7.5	4.3	staircase
2o	4:7	12.2, 11.4	26.3	flat

**Figure 3.** H-bonded layer in the host–guest complexes of **I**. Benzyl groups are omitted for the sake of clarity.

guest ratio and unit cell lengths are approximately the same. The host–guest interactions are depicted in a series of figures by omitting the acid moieties and NH₂(CH₂)₂ fragments for the sake of clarity.

Host–Guest Complexes of I. The H-bonded sheets (Figure 3) are composed of two cyclic rings of 24 atoms (5 H-bonds) and 20 atoms (5 H-bonds), respectively. Tetrameric aggregates of TMA propagate throughout the layer. The H-bonded layers are corrugated but there is considerable variation in the degree of corrugation. All the complexes except **1j** exhibit crystallographically identical packing in adjacent layers; i.e., they are related by translation. The interlayer separations range from 9.3 to 12.2 Å, and except for **1j**, the unit cell lengths of the complexes are multiples of $\sim 12 \times 17 \times 21$ Å.

1c–1f form host–guest complexes with 1:1 stoichiometry. In **1c** and **1d**, the layers are less corrugated than in **1e** and **1f** (Figure 4). Benzyl groups orient to form cavities that are occupied by dimers of guest molecules (Figure 5). **1g** and **1h** generate host–guest complexes in 4:5 ratio and the H-bonded layers are corrugated (Figure 6A). The asymmetric unit also

**Figure 4.** Supramolecular laminates (a) **1d** (viewed along short axis) and (b) **1e** (viewed along long axis). Note the difference in corrugation between **1d** and **1e**. Guest molecules are presented in space-filling mode.**Figure 5.** Aromatic interactions between the benzyl groups and guest molecules in **1d**. Note that there are dimers of guest molecules.

contains a 4:5 ratio of host to guest. Such a large asymmetric unit is exceptional in the context of small-molecule crystallography but occurs in several of the other structures reported herein. The packing of the benzyl groups is quite different from **1c** to **1f** and results in alternately small and large cavities (Figure 6B). The small cavities are occupied by monomers of guest molecules that interact with the benzyl moieties via C–H \cdots π interactions. The large cavities are occupied by trimers of guest molecules that exhibit C–H \cdots π interactions among themselves and with benzyl moieties.

1i forms a corrugated H-bonded layer that is solvated by EtOH (Figure 7A). The distance between two consecutive solvent molecules is 25 Å, which is equal to half of the length of the short axis (~ 50 Å or 3×17 Å). Unlike **1b** and **2a**, the EtOH molecules are not integrated into the H-bonded layer.

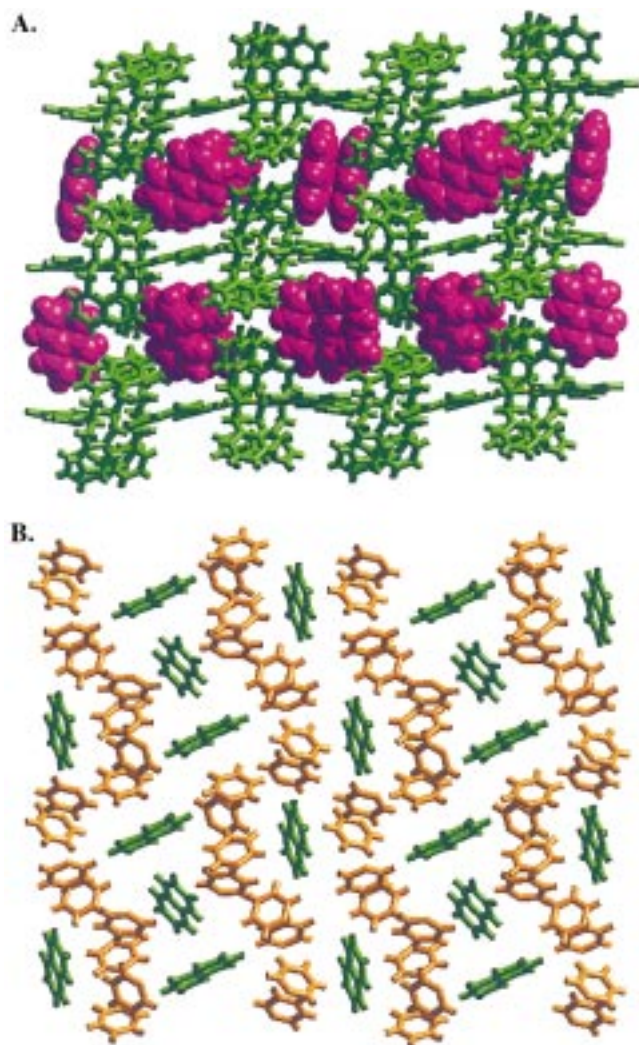


Figure 6. (A) Supramolecular laminate **1g** (viewed along short axis). (B) C–H... π interactions between benzyl groups and guest molecules in **1g**. Note that there are monomers and trimers of guest molecules.

Rather, they cling to the surface of the layer via O–H...O H-bonds. The benzyl groups generate alternately small and large cavities (Figure 7B). The small cavities are occupied by single veratrole molecules, whereas the large cavities are occupied by adducts of veratrole and EtOH. The EtOH molecules form C–H...O hydrogen bonds with the CH₃ group of the veratrole molecules (C...O, 3.537 Å; H...O, 2.766 Å; C–H...O, 137.8°).

In **1j**, alternate layers are different. One layer contains anisole and H₂O molecules whereas the next layer contains no guests and is sustained by interdigitation of benzyl groups (Figure 8). The H₂O molecules are not part of the H-bonded network. Rather, they attach via OH...O hydrogen bonds. Anisole molecules are surrounded by benzyl groups.

Host–Guest Complexes of II. The H-bonded sheets are similar to those observed in **2b** (Figure 2d), and they are either flat or corrugated. The interlayer separations range from 7.5 to 12.9 Å and the unit cell lengths are multiples of $\sim 12 \times 17 \times 21$ Å except for **2j**, **2m**, and **2n**.

In complexes **2c–2j** the host–guest ratio is 1:1. **2e**, **2g**, **2h**, and **2i** form flat H-bonded layers while **2c**, **2d**, **2f**, and **2j** form corrugated H-bonded layers (Figure 9). In complex **2c**, *N,N*-dibenzylamine molecules are present as guests, and interestingly, the N–H moiety does not form a hydrogen bond. This implies

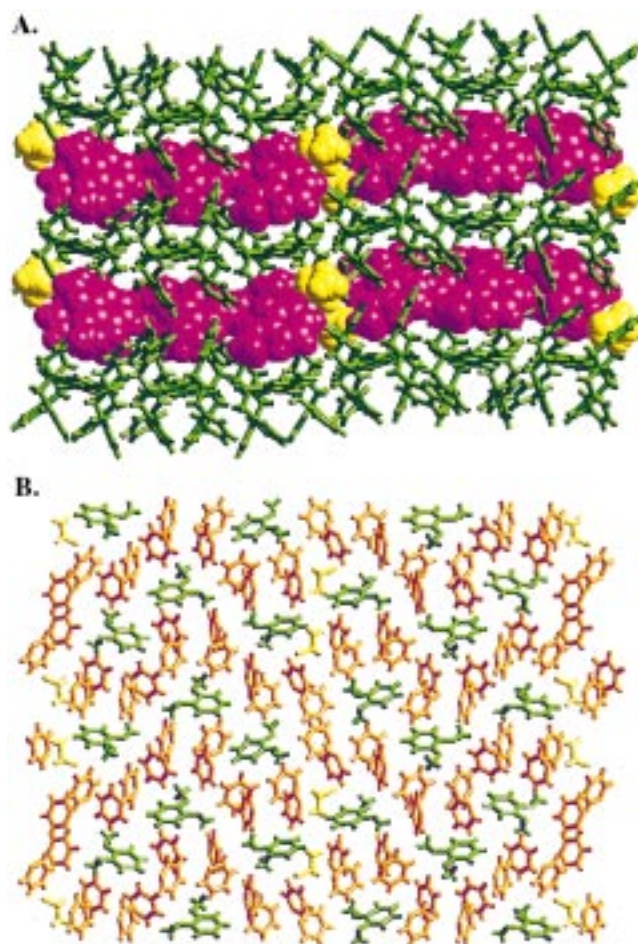


Figure 7. (A) Supramolecular laminate **1i** (viewed along long axis). Note that the solvent molecule (yellow) repeats every three guest molecules. (B) C–H... π interactions between benzyl groups (orange) and guest molecules (green) in **1i**.

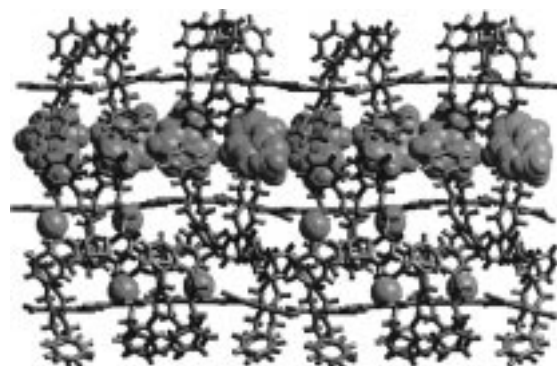


Figure 8. Supramolecular laminate **1j** (viewed along short axis). Note that alternate layers are different, containing anisole or water molecules, respectively.

that the sum of the C–H... π interactions is greater than a single N–H...O H-bond. The distance between the N-atoms of the guest molecule and its nearest neighbor, a C-atom, is 4.065 Å. **2c** exhibits the longest interlayer separation (12.9 Å) of all the complexes reported herein. The benzyl groups in **2f–2j** form tetrameric aggregates via C–H... π interactions, and these tetrameric aggregates interact with guest molecules in a herringbone arrangement (Figure 10A). In **2c** and **2d**, the benzyl groups form cavities which are occupied by dimers of guest molecules (Figure 10B). **2e** exhibits two symmetry-independent dimers. Therefore, there are two symmetry-independent dimers

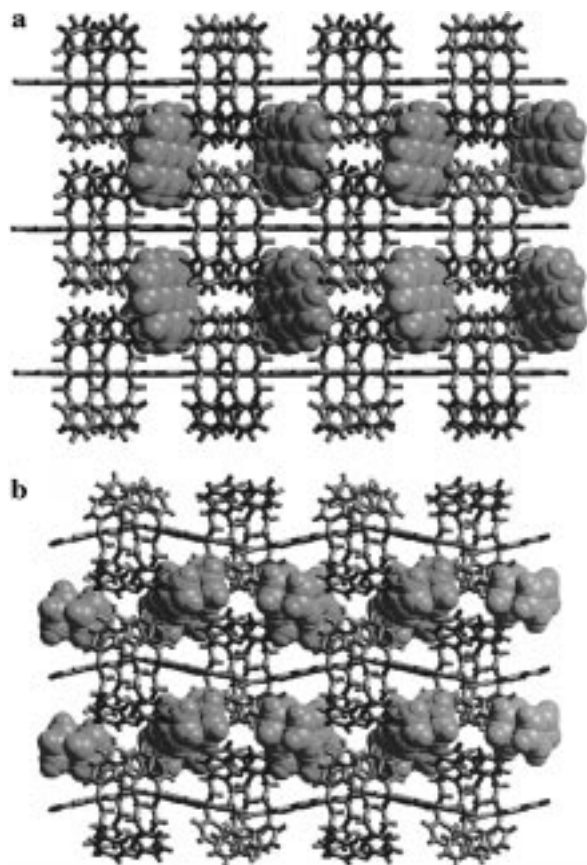


Figure 9. Supramolecular laminates (a) **2i**, flat H-bonded sheets, and (b) **2j**, corrugated H-bonded sheets.

of guest molecules (Figure 10C) with interplanar angles of 31.8 and 93.7°, respectively.

2k and **2l** form host–guest complexes with 1:1.5 stoichiometry and exhibit flat H-bonded layers (Figure 11). In both complexes, benzyl groups form tetrameric aggregates similar to **2f–2j** but the aggregates align differently with guest molecules, as illustrated in Figure 11b.

2m forms a 3:4 host–guest complex, and the length of the long axis of the unit cell is tripled (63 Å). The H-bonded sheets are corrugated (Figure 12a), and the benzyl groups generate two types of cavity, which are occupied by dimers and trimers of guest molecules, respectively (Figure 12b). The dimers and trimers occupy the cavities in such a way that two consecutive columns of trimers are followed by a column of dimers. The distance between the consecutive columns of dimers is 31.5 Å, which is equal to the half of the length of the long axis (~63 Å or 3×21 Å).

2n is a host–guest complex with 4:1 stoichiometry. The unit cell lengths and crystal packing differ noticeably from the other complexes, but the H-bonding pattern remains intact. The geometry of the H-bonded layer is neither flat nor corrugated. Rather, it can be described as a staircase motif (Figure 13). Interdigitation of benzyl groups occurs which results in the shortest interlayer separation, 7.5 Å.

2o forms a 4:7 host–guest complex and exhibits flat H-bonded layers. Therefore, there are 19 organic residues in the asymmetric unit. To our knowledge, there are no organic crystal structures in the CSD with this number of residues in the asymmetric unit. The packing in neighboring layers is significantly different (Figure 14) as guest molecules alternate between perpendicular (edge-to-face stacking) and parallel (face-

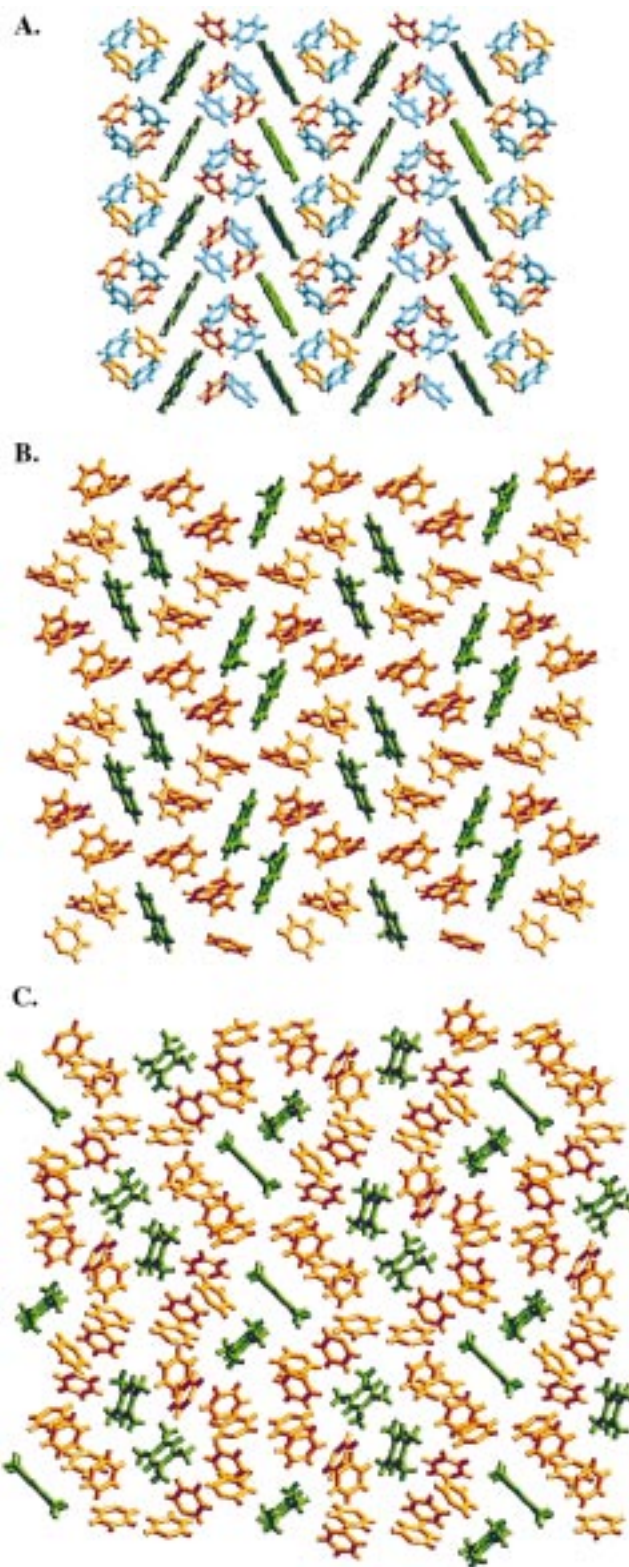


Figure 10. C–H... π interactions between the benzyl groups (orange or blue) and guest molecules (green) in (A) **2i**, (B) **2d**, and (C) **2e**. Note the herringbone type of packing between the tetrameric aggregates of benzyl groups and guest molecules in **2i**.

to-face stacking) orientation with respect to the H-bonded sheet. The benzyl groups form tetrameric aggregates when the nitrobenzene molecules are perpendicular to the H-bonded sheet (Figure 14a), whereas they form cavities that are occupied by dimers of nitrobenzene when the nitrobenzene molecules are parallel to the H-bonded sheet (Figure 14b).

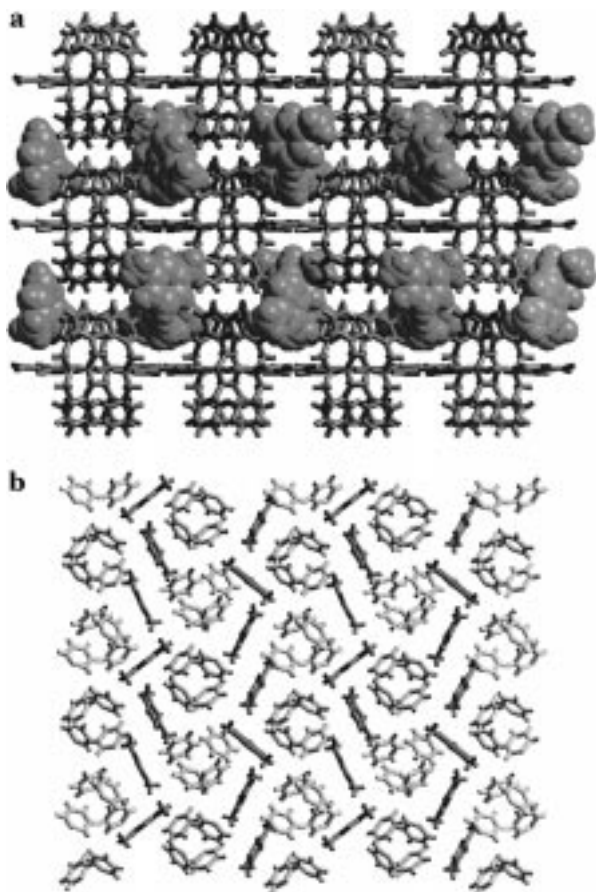


Figure 11. (a) Supramolecular laminates **2l** (viewed along short axis). (b) C-H... π interactions between the benzyl groups and guest molecules in **2l**. Compare (b) with Figure 10a.

Guest Exchange. A number of guest exchange reactions were conducted. For example, if crystals of **2l** are placed in pure veratrole under ambient conditions, they became opaque after one week and IR spectra are identical to a sample of **2h**. The IR spectra are unambiguous because of the characteristic peak of veratrole at 1253 cm^{-1} (C–O stretch). All samples eventually lose guest if they are exposed to the atmosphere for long periods of time or subjected to vacuum or heat. The apohosts readily adsorb guest molecules from solution.

Conclusions

The supramolecular laminates **I** and **II** incorporate a wide range of aromatic guest molecules or, even more importantly, supramolecular complexes of organic molecules. It seems reasonable to assert that their affinity for aromatic molecules is based upon the ability of the pendant benzyl moieties to engage in C–H... π interactions with the guest molecules. That guest molecules of varying size and shape are enclathrated is a reflection of two factors. First, the nature of laminated architectures is such that there is, in principle, an infinite surface area available for guests. Second, the structure is inherently flexible in a number of ways: (i) variation of interlayer separations from 7.5 to 12.9 Å occurs; the H-bonded networks are robust but flexible (i.e., corrugated or flat; the inherent torsional flexibility of the benzyl groups (torsion angles 1–2–3–4 vary between 35 and 140°) manifests itself by allowing

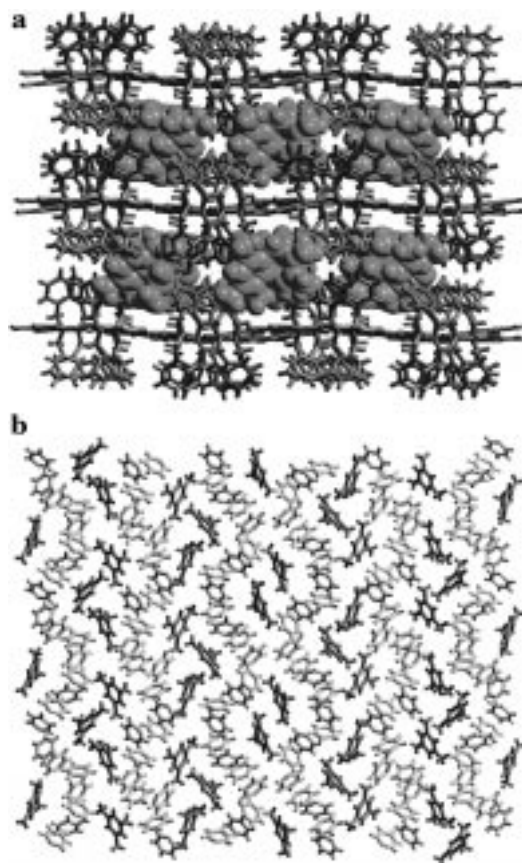
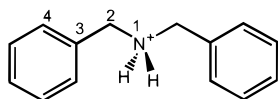


Figure 12. (a) Supramolecular laminates **2m** (viewed along short axis). Note the high degree of corrugation. (b) C–H... π interactions between the benzyl groups and guest molecules in **2m**. Note that the dimers and trimers of guest molecules exist in a 1:2 ratio.

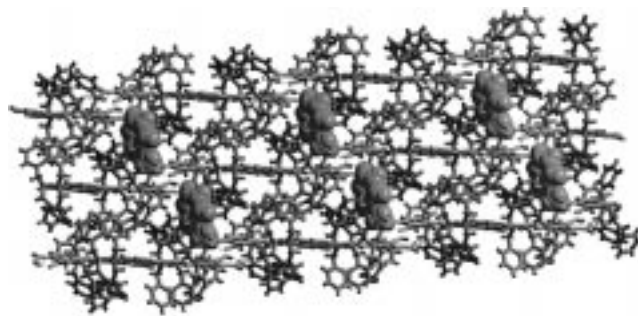


Figure 13. Supramolecular laminates **2n** with staircase geometry of the H-bonded layers. Note that interdigitation occurs as well as incorporation of guest molecules.

the generation of a wide range of cavity and/or channel geometries. The ability of the supramolecular laminates to form similar crystalline structures with such a wide range of guests can therefore be rationalized.

That the guest molecules can be easily removed by heat to afford a stable amorphous apohost or exchanged by contact with solvent that is rich in another guest molecule means that such compounds are potentially useful as functional materials. Indeed, when combined with their low-cost, facile supramolecular synthesis, chemical stability, and modular nature, the new compounds described herein have potential applications in the context of separations, sensors and general purpose adsorbents.

In summary, the compounds reported herein represent, to our knowledge, the second example¹³ of a series of simple laminated

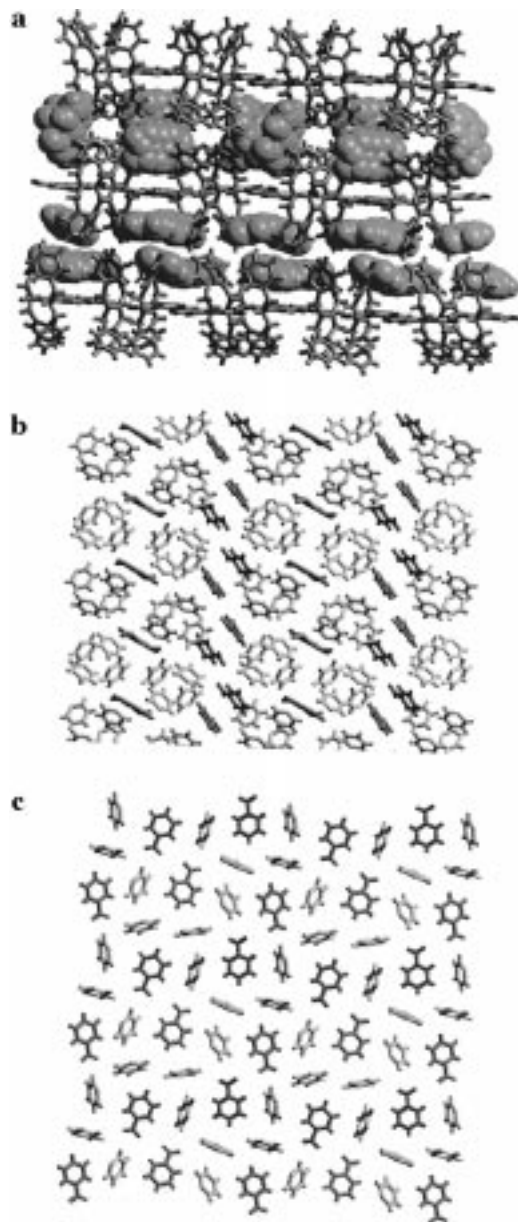


Figure 14. (a) Supramolecular laminates of **2n** in which guest molecules have alternating packing modes (viewed along short axis). C—H $\cdots\pi$ interactions between the benzyl groups and guest molecules are illustrated (b) when the guest is perpendicular to the H-bonded layer and (c) when the guest is parallel to the H-bonded layer. Compare (b) with Figure 10a and Figure 11b.

salts that mimic clays in their ability to intercalate guest molecules. We note that these compounds are sustained entirely by noncovalent interactions, are inherently hydrophobic and, because of their 2D structures and flexibility, have a generic affinity toward intercalation of aromatic molecules. A key feature is that, unlike zeolite mimics, they are selective for chemical type more than size and shape. They therefore complement the stronger shape and size selectivity of 3D structures. We continue to investigate the structural and functional properties of laminated architectures based upon exofunctional anions such as those described herein.

Experimental Section

Preparation of Crystals. **I** and **II** were synthesized by reacting 1 equiv of H₃TMA or H₃TML with 2 equiv of *N,N*-dibenzylamine in the presence of excess guest. Salts **1a** and **2a** were formed and crystallized from EtOH while **1b** and **2b** were formed and crystallized from MeOH and MeCN, respectively. Crystals of the host–guest complexes (**1c–1j**, **2c–2o**) were prepared by crystallizing H₃TMA or H₃TML with 2 equiv of *N,N*-dibenzylamine from MeOH or EtOH, respectively, in the presence of excess guest (5 equiv for solid guests, 10 equiv for liquid guests). The ratios of guest molecules found in the isolated host–guest complexes are presented in Table 2. The mp's of host–guest complexes of **I** are >300 °C whereas those of complexes **II** are in the range of 150–170 °C.

X-ray Crystal Structure Determinations. Single-crystal X-ray diffraction data for the complexes **1a**, **1e–1j**, **2b**, **2d–2h** and **2j–2o** were collected on a Siemens SMART/CCD diffractometer equipped with an LT-II low-temperature device. Diffracted data were corrected for absorption using the SADABS²³ program. SHELXTL²⁴ was used for the structure solution and refinement was based on *F*². The diffraction data for complexes **1b–1d**, **2a**, **2c**, and **2i** were collected on an Enraf-Nonius CAD4 diffractometer at 290 K using the ω scan mode, and the crystallographic calculations were carried out using the NRCVAX²⁵ program package locally implemented on an 80486-based compatible computer. All non-hydrogen atoms were refined anisotropically. Acid protons were located and refined with isotropic thermal parameters whereas the remaining hydrogen atoms of the host were fixed in calculated positions and refined isotropically with thermal parameters based upon the corresponding C-atoms [*U*(H) = 1.2*U*(eq(C))]. A general crystallographic problem became apparent with the guest molecules. Their presence in large channels or cavities means that they are susceptible to disorder or high thermal motion, even at low temperature. However, guest molecules were located successfully in all compounds and disorder was found in **1c** and **2o**. Non-hydrogen atoms of the guests molecules were refined anisotropically. However, the high thermal motion afforded relatively high *R*-factors, in some cases >0.10. In compound **2o**, one of the nitrobenzene guest molecules is disordered over two sites with 0.5 occupancy whereas **1c** contains disordered guests and benzyl groups. In hindsight, it seems remarkable that these structures are as tractable as they were. We attribute this at least partly to the ability of CCD X-ray diffractometers to readily resolve doubling and tripling of unit cell lengths. In almost all cases, the guest molecules were responsible for the large asymmetric units present in the compounds reported herein. Interplanar distances are evaluated by calculating the distance between the mean planes of adjacent layers. Pertinent crystallographic data are given in Table 1. Fractional coordinates and anisotropic displacement parameters have been deposited as Supporting Information.

Acknowledgment. We gratefully acknowledge the Environmental Science and Technology Alliance Canada (ESTAC) and the Natural Sciences and Engineering Research Council of Canada (NSERC) for providing financial support.

Supporting Information Available: Tables of crystal structures refinement data, positional parameters, and bond lengths and angles are available (470 pages, print/PDF). See any current masthead page for ordering information and Web access instructions.

JA973738Y

(23) Sheldrick, G. M. *SADABS*; University of Gottingen, 1996.

(24) Sheldrick, G. M. *SHELXTL, Release 5.03*; Siemens Analytical X-ray Instruments Inc.: Madison, WI, 1994.

(25) Gabe, E. J.; Page, Y. Le.; Charland, J.-P.; Lee, F. L.; White, P. S. *J. Appl. Crystallogr.* **1989**, *22*, 384.